Biochemical and Biophysical Research Communications 373 (2008) 140–145

Contents lists available at ScienceDirect

Biochemical and Biophysical Research Communications

journal homepage: www.elsevier.com/locate/ybbrc

Identification and characterization of a putative lipopolysaccharide-induced TNF-α factor (LITAF) homolog from Singapore grouper iridovirus

Xiaohong Huang, Youhua Huang, Jie Gong, Yang Yan, Qiwei Qin *

State Key Laboratory of Biocontrol, School of Life Science, Sun Yat-sen University, 135, West Xingang Road, Guangzhou 510275, China

ARTICLE INFO

Article history:
Received 16 May 2008
Available online 11 June 2008

Keywords:
Iridovirus
Singapore grouper iridovirus (SGIV)
Lipopolysaccharide-induced TNF-α factor (LITAF)
Apoptosis

ABSTRACT

Lipopolysaccharide-induced TNF-α factor (LITAF), a transcription factor, can regulate tumor necrosis factor alpha (TNF-α) transcription. Here, a novel LITAF homolog encoded by Singapore grouper iridovirus (SGIV LITAF) was identified and characterized. The putative SGIV LITAF encoded a protein of 104 amino acids (aa) with a predicted molecular mass of 11.6 kDa. Reverse transcription-PCR (RT-PCR) and Western blot analyses of SGIV-infected cells revealed that SGIV LITAF was an early viral gene. Subcellular localization and immunofluorescence assay revealed that SGIV LITAF expression was distributed predominantly in the cytoplasm, associated with mitochondria. Overexpression of SGIV LITAF induced apoptosis, as shown by increased apoptotic bodies, depolarization of mitochondrial membrane potential ($\Delta\Psi_m$) and activation of caspase-3. Furthermore, NF-κB and NFAT activities were increased in cells expressing SGIV LITAF. This is the first report of the identification and characterization of a viral LITAF homolog involved in virus–host interaction.

Iridoviruses are large DNA viruses that infect only invertebrates and poikilothermic vertebrates. The family *Iridoviridae* is divided into five genera: *Ranavirus*, *Lymphocystivirus*, *Megalocytivirus*, *Iridovirus*, and *Chloriridovirus* [1]. Singapore grouper iridovirus (SGIV) was first isolated from the brown-spotted grouper, and was characterized as a novel ranavirus [2,3]. Genome sequence analysis of SGIV showed that some potential viral gene products, including tumor necrosis factor (TNF)-related cytokines, were involved in virus–host interactions and immune evasion [4]. Although the TNF superfamily of cytokines are critical for mounting innate and adaptive immune responses against foreign pathogens by regulating cell death and survival, viruses have evolved a variety of strategies to regulate the effects of death receptor signaling in the infected cells themselves, aiding the progression of viral replication and dissemination [5,6]. Investigation of the SGIV-encoded TNF-related cytokines will contribute to the understanding of the mechanism of virus pathogenesis.

Lipopolysaccharide (LPS) is a potent stimulator of monocytes and macrophages, causing secretion of tumor necrosis factor alpha (TNF-α) and other pro-inflammatory cytokines. Recently, a novel transcription factor, LPS-induced TNF-α factor (LITAF), was cloned and characterized from the human macrophage cell line THP-1 following treatment with LPS [7]. LITAF was found to affect TNF-α expression by formation of a complex with STAT6 [8], and also plays a role in the regulation of various inflammatory cytokines by separating from NF-κB [9]. Subsequently, several LITAF homologs have been cloned and identified from other species such as mouse, zebrafish, chicken, and Pacific oyster [10–13]. However, there have been no further studies on LITAF homologs from viruses, except for predictions based on the genome sequences [14]. In the present study, we cloned a putative viral LITAF homolog from SGIV (SGIV LITAF) and investigated its subcellular localization, transcription, and cytotoxic effects on fish cells.

Materials and methods

Virus and cells. Propagation of SGIV and isolation of the viral genomic DNA were performed as described previously [3]. Grouper embryonic cells (GP) were grown in Eagle's minimum essential medium containing 10% fetal bovine serum at 25 °C.

Gene cloning, plasmid construction, and computer-assisted analysis. The full length of SGIV LITAF (ORF136) was cloned by PCR from SGIV genomic DNA using a pair of primers, P1/P2 (P1, 5′-TTG GATCCGCGCACATGTACCCT-3′; P2, 5′-ATCTCGAGCCCCGAACGTTA ATTATACA-3′). The fragment produced was then cloned into prokaryotic vector pET32-a (+) to obtain plasmid pET-LITAF. Two other pairs of primers, P3/P4 (P3, 5′-TTCTCGAGCGCACATGTACCCTGTAT-3′; P4, 5′- GTGGATCCTACAATTTTATAAACGGCGA-3′) and P5/P6 (P5, 5′-ACGAATTCACATGGACCCTGTATTGAA-3′; P6, 5′-ATCTCGAGCCCC GAACGTTAATTATACA-3′), were also used to amplify the SGIV LITAF gene with the introduced restriction enzyme sites, then the fragments were cloned into eukaryotic vectors pEGFP-N3 and pcDNA3.1(+) to obtain plasmids pEGFP-LITAF and pcDNA-LITAF.

* Corresponding author. Fax: +86 20 39332939.
E-mail address: lssqinqw@mail.sysu.edu.cn (Q. Qin).

0006-291X/$ - see front matter © 2008 Elsevier Inc. All rights reserved.
doi:10.1016/j.bbrc.2008.06.003

The different constructs were confirmed by sequencing. Alignment of amino acid sequences was carried out using Clustal X 1.83 and edited using the GeneDoc program.

Prokaryotic expression, purification, and antibody preparation. The recombinant plasmid pET-LITAF was transformed into *Escherichia coli* BL21 cells and the fusion protein was expressed under induction conditions of exposure to isopropyl 1-thio-β-D-galactopyranoside (1 mM) at 37 °C for 4 h. The fusion protein was purified according to the protocol supplied with the HisBind purification kit (Novagen). The purified protein was injected into mouse subcutaneously at 7-day intervals. The antiserum was collected after the fifth immunization and used for the following immunoassay.

RT-PCR and Western blot analysis. For transcriptional analysis, GP cells were infected with SGIV at a multiplicity of infection (MOI) of approximately 0.5. Total RNA was isolated from mock- and virus-infected cells at 2, 4, 6 10, 16, 24, 36, and 48 h postinfection (p.i.) using Trizol Reagent (Invitrogen) according to the manufacturer's protocol. After the RNA had been digested with RNase-free DNase, 1 μg of RNA from each time point was transcribed by Moloney Murine Leukemia Virus Reverse Transcriptase (M-MLV RT) and random primers to synthesize the first strand cDNA. PCR was then performed using gene-specific primers, P7/P8 (P7, 5′-AGTTTTTC CACGACACGG-3′; P8, 5′-GAATGGGAGACCTCTTTACT-3′). Detection of β-actin mRNA was used as an internal control.

To examine the protein expression pattern, Western blot analysis was performed with total proteins that had been collected from SGIV-infected cells. The anti-SGIV LITAF serum was used as the primary antibody at a dilution of 1:1000, and the secondary antibody was goat anti-mouse IgG coupled to alkaline phosphatase at a dilution of 1:10,000 (Sigma). Simultaneously, internal controls were performed by detecting β-actin protein. In addition, cycloheximide (CHX) and cytosine arabinofuranoside (AraC) were used to classify the temporal expression of SGIV LITAF during infection. Briefly, GP monolayer cells were pretreated with 50 μg/ml CHX or 100 μg/ml AraC for 1 h prior to and throughout the SGIV infection. CHX or AraC-pretreated cells were mock-infected or infected with approximately 0.5 MOI SGIV, then harvested at 6 h p.i. and 48 h p.i., respectively. The protein extracts from the samples were subjected to Western blot analysis as described above.

Cell transfection. Transfection was performed using the Lipofectamine 2000 reagent according to the manufacturer's instructions (Invitrogen). Briefly, cells were grown to 90% confluence in 24-well plates. Lipofectamine 2000 and plasmids were mixed for 25 min before transfection. Then cells were incubated with the mixture for 6 h at 25 °C, and cultured with fresh medium for further analysis.

Subcellular localization analysis. After transfection with pEGFP-LITAF or pEGFP-N3 for 48 h, cells were washed with PBS and fixed with 4% paraformaldehyde for 30 min, and then stained with 6-diamidino-2-pheny-lindole (DAPI) for 15 min. Finally, cells were mounted with 50% glycerol, and observed under fluorescence microscopy (Zeiss). To increase the accuracy of detection of the subcellular location of SGIV LITAF, pDsRed2-Mito was cotransfected with pEGFP-LITAF. For immunofluorescence localization, GP cells were either mock-infected or infected at 0.5 MOI for 18 h and then fixed with 4% paraformaldehyde. The coverslips were blocked by bovine serum albumin (BSA) for 30 min. Cells were incubated with anti-SGIV LITAF antiserum (1:100) for 1 h. After washing in PBS, a secondary antibody conjugated with FITC (Pierce) was incubated for a further hour. Cellular and viral DNA was then labeled with DAPI, followed by fluorescence microscopic observation.

Hoechst staining. To detect the effects of SGIV LITAF expression on the fish cells, pcDNA-LITAF or pcDNA 3.1 was transfected. Following transfection for 48 h, cells were washed with PBS, and then stained with Hoechst 33342 at a final concentration of 1 μg/ml to

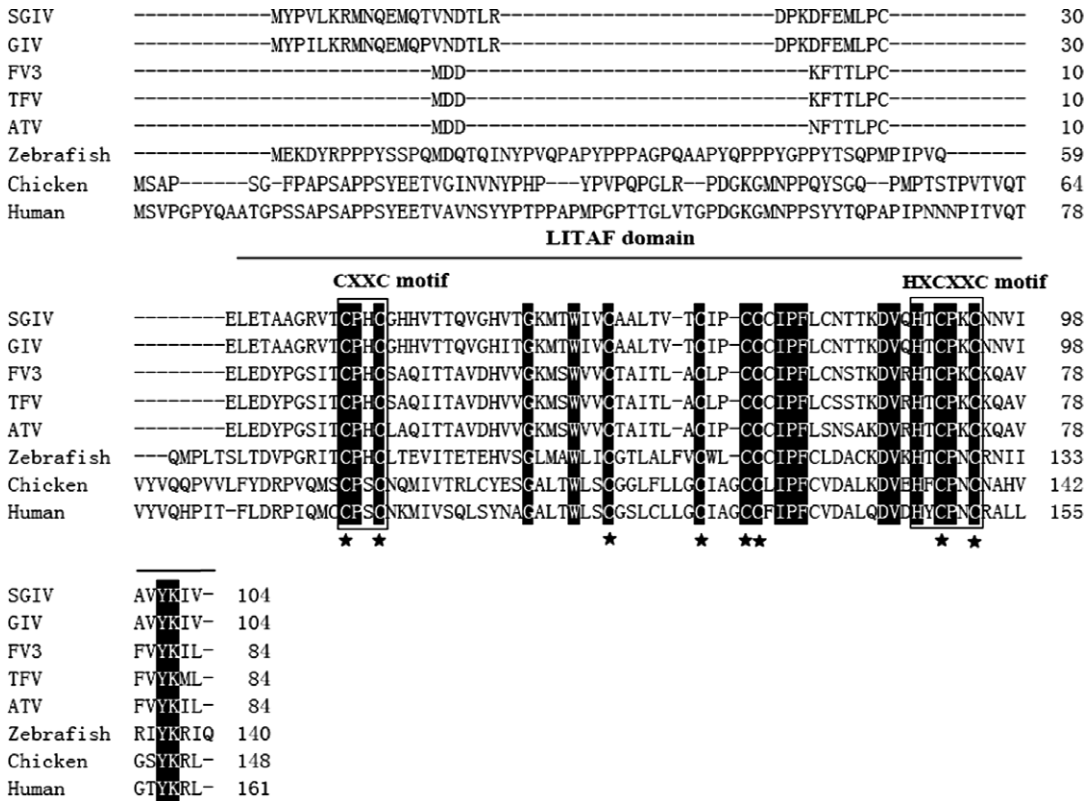

Fig. 1. Multiple amino acid sequence alignment of LITAF homologs from SGIV and selected species. Identical amino acids are highlighted by black boxes and the conserved cysteines (C) are indicated by asterisks under the alignment. The characteristic domains are shown by rectangles. The predicted LITAF domain, which contains the CXXC and HXCXXC motifs, is indicated above the sequence.

visualize nuclear morphology. The cells were observed under fluorescence microscopy.

JC-1 analysis. Examination of mitochondrial membrane potential ($\Delta\Psi_m$) was carried out using JC-1. After 48 h transfection, cells were washed with PBS, and incubated with JC-1 dye in incubation buffer for 20 min. Cells were then washed in incubation buffer and placed in fresh medium. Cells were observed under fluorescence microscopy. The data were collected simultaneously at emissions of 530 and 590 nm, respectively.

Analysis of caspase-3 activity. To investigate the caspase-3 activity after SGIV LITAF expression, Ac-DEVD-AMC was used. After 48 h transfection, pcDNA3.1 or pcDNA-LITAF transfected cells were collected. The detection of caspase-3 activity was performed as described previously [15]. The data were expressed as the -fold increase compared with the corresponding values of caspase activity in lysates of empty vector transfected cells.

Reporter gene assays. The activation of transcript factors NF-κB and NFAT in SGIV LITAF transfected cells was also measured using a NF-κB and NFAT dependent luciferase reporter construct (NF-κB -luc and NFAT-luc, Clontech). Briefly, GP cells were cotransfected with 80 ng of NF-κB-luc or NFAT-luc, 20 ng of cytomegalovirus β-galactosidase reporter construct, and pcDNA-LITAF. After incubation for 72 h, cells were harvested and analyzed for luciferase expression using the luciferase assay system, following the manufacturer's instruction. Samples were also assayed for β-galactosidase activity using a β-galactosidase enzyme assay system to normalize for transfection efficiency.

Results

Identification and sequence analysis of the SGIV LITAF gene

The annotation of SGIV ORF136 (YP_164231) revealed a previously uncharacterized virus LITAF homolog. The coding region of SGIV ORF136 is 315 base pairs (bp) in length, and encoded a 104-amino acid (aa) peptide with a predicted molecular weight of 11.6 kDa. The amino acid alignment indicated that SGIV ORF136 contained a conserved LITAF domain with CxxC and (H)xCxxC knuckles and eight conserved cysteine residues at the carboxyl terminus. GenBank searches of protein databases revealed that SGIV ORF136 is shared by all ranaviruses whose complete genomes have been sequenced (Fig. 1). SGIV ORF136 showed high amino acid sequence identity with ranaviruses, ranging from 97% with grouper iridovirus (GIV) (AAV91101) to 60% with tiger frog virus (TFV) (ABB92333). In contrast, SGIV ORF136 showed lower identities of 47%, 38%, and 35% with zebrafish (XP_687915), chicken (NP_989598) and human (NP_004853) LITAF, respectively. Therefore, SGIV ORF136 was found to be novel and was named SGIV LITAF.

Expression of SGIV LITAF in SGIV-infected cells

To follow the temporal transcription of SGIV LITAF in vitro, RT-PCR was performed using SGIV-infected cells at different infection stages. The 295 bp SGIV *LITAF* gene-specific fragment was detected at 4 h p.i., and high-level transcription continued until 48 h p.i. (Fig. 2A). The expression of SGIV LITAF protein was also examined using the prepared antiserum, which was specific for the SGIV LITAF protein (data not shown). Western blot analysis showed that a specific immunoreactive band of approximately 11 kDa was observed at 6 h p.i., and the signal intensity of both bands increased with time up to 48 h p.i. No immunoreactive band was detected in mock-infected control cells (Fig. 2B).

The expression of SGIV LITAF under drug pressure was investigated using Western blot analysis. As shown in Fig. 2C, the 11 kDa protein band was detected in the infected cells treated with AraC, and its content was less than that in the untreated cells. However, the specific band was not detected after treatment with CHX, indi-

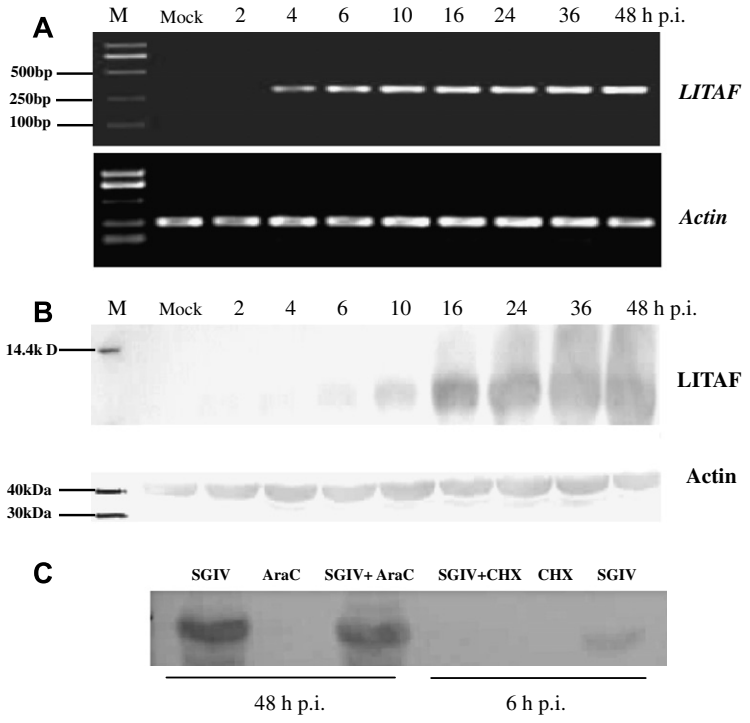

Fig. 2. Temporal expression pattern of SGIV LITAF in SGIV-infected GP cells. (A) RT-PCR examination of SGIV LITAF transcription. (B) Western blot analysis of LITAF expression. Total RNAs and proteins were prepared from SGIV-infected cells at different times p.i.; β-actin was detected under the same conditions as a positive control. DNA and protein markers are in lane M on the left. (C) Western blot detection of SGIV LITAF expression in the absence or presence of CHX or AraC.

cating that SGIV LITAF belongs to the early class of genes activated during in vitro infection.

Subcellular localization of SGIV LITAF

To examine the subcellular localization of SGIV LITAF, a recombinant plasmid, pEGFP–LITAF, was constructed and transfected into GP cells. pEGFP-LITAF transfected cells were rounded and the green fluorescence was aggregated in the cytoplasm close to the nucleus. Fluorescence was also observed in the plasma membrane in some transfected cells (Fig. 3A, lower row), while the green fluorescence signal was distributed in both cytoplasm and nucleus in the control cells (Fig. 3A, upper row). To further evaluate the precise location of SGIV LITAF, pDsRed2-Mito, a mitochondria-specific marker, was used. The results showed that the green fluorescence was partially co-localized with red fluorescence, indicating that SGIV LITAF was associated with the mitochondria (Fig. 3B).

The intracellular location of SGIV LITAF was also determined in infected cells by immunofluorescence using anti-SGIV LITAF antiserum. As shown in Fig. 3B, SGIV LITAF localized primarily in the cytoplasm, and appeared to aggregate toward the viral factories in infected cells. In some infected cells, green fluorescence was present in the plasma membrane. No fluorescence signal was detected in the mock-infected cells (Fig. 3C, upper row). We also observed distorted and condensed nuclei in SGIV-infected cells, whereas intact nuclei were seen in mock-infected cells.

Effects of SGIV LITAF expression on fish cells

To understand the effect of SGIV LITAF expression on fish cells, morphological and biochemical changes in pcDNA-LITAF

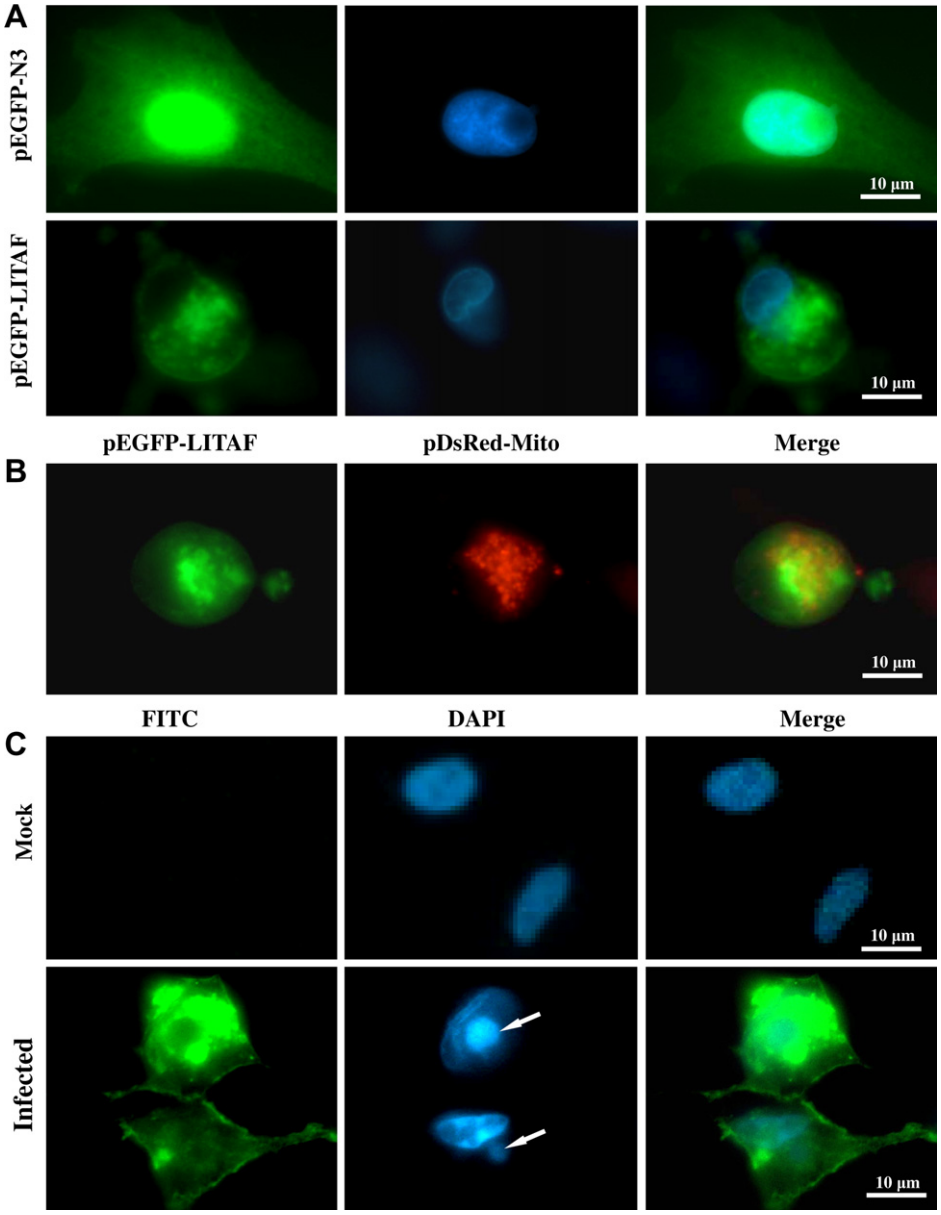

Fig. 3. Intracellular localization of SGIV LITAF. (A) Intracellular localization of SGIV LITAF by fluorescence microscopy. GP cells were transfected with pEGFP-N3 (upper row) or pEGFP-LITAF (lower row). Blue images show the location of the nucleus, stained by DAPI. (B) Subcellular localization of SGIV LITAF by cotransfecting with pDsRed2-Mito. Red images show the location of mitochondria (Mito). (C) Expression of SGIV LITAF in SGIV-infected cells by immunofluorescence detection. The arrows indicate viral factories. (For interpretation of the references to color in this figure legend, the reader is referred to the web version of this paper.)

transfected cells were investigated. The expression of SGIV LITAF was confirmed after transfection by the presence of the specific protein band on Western blot analysis using anti-SGIV LITAF antiserum (Fig. 4A). Hoechst staining analysis showed that many apoptotic bodies were present in pcDNA-LITAF transfected cells, while intact nuclei were observed in pcDNA transfected cells (Fig. 4B).

Outer $\Delta\Psi_m$ is one of the important steps that occurs during apoptosis. To explore whether SGIV LITAF expression could induce the depolarization of $\Delta\Psi_m$, JC-1 was used. In non-apoptotic cells, JC-1 accumulates as aggregates in the mitochondria, resulting in red fluorescence. In contrast, in apoptotic and necrotic cells, JC-1 exists in monomeric form and stains the cytosol green. As shown in Fig. 4C, in pcDNA transfected cells, the JC-1 dye accumulates in the mitochondria and appears bright red. However, in pcDNA-LITAF transfected cells, the red fluorescent aggregates were dispersed, and green fluorescence was observed throughout the cytosol. The results implied that SGIV LITAF expression could induced the collapse of $\Delta\Psi_m$.

Caspase-3 is a key mediator of apoptosis. To evaluate the possible involvement of downstream effector caspases, the activity of caspase-3 was detected after SGIV LITAF transfection. As shown in Fig. 4D, fluorometric analyses revealed a 4.4-fold increase in caspase-3 activity at 48 h post-transfection in comparison to the empty vector transfected cells. In CHX treated cells, a 6.3-fold increase in caspase-3 activity was recorded.

Furthermore, changes in the activation of NF-κB and NFAT were detected in pcDNA-LITAF transfected cells. As shown in Fig. 4E, the luciferase activity of NF-κB and NFAT increased in pcDNA-LITAF transfected cells compared with that in the pcDNA3.1 transfected cells. To normalize the transfection efficiency, the expression level of β-galactosidase was also investigated, and no differences were found between pcDNA-LITAF and empty vector transfected cells (data not shown). The data suggested that SGIV LITAF expression activates NF-κB and NFAT dependent transcription.

Discussion

LITAF is an important transcriptional factor that has been discovered in all taxonomic groups from vertebrates, such as mammals, birds, and fish, to invertebrates [7,13]. LITAF can bind to the TNF-α promoter to regulate its expression and may play an important role in diverse host responses [8,9]. To our knowledge, no LITAF homologs had been previously identified from viruses. Recently, the complete genome sequences of 12 iridoviruses have been published [14]. Computer assisted analysis showed that SIGV ORF136 contained a typical LITAF-like domain similar to other known LITAF proteins. Significantly, viral LITAF (vLITAF) homologs

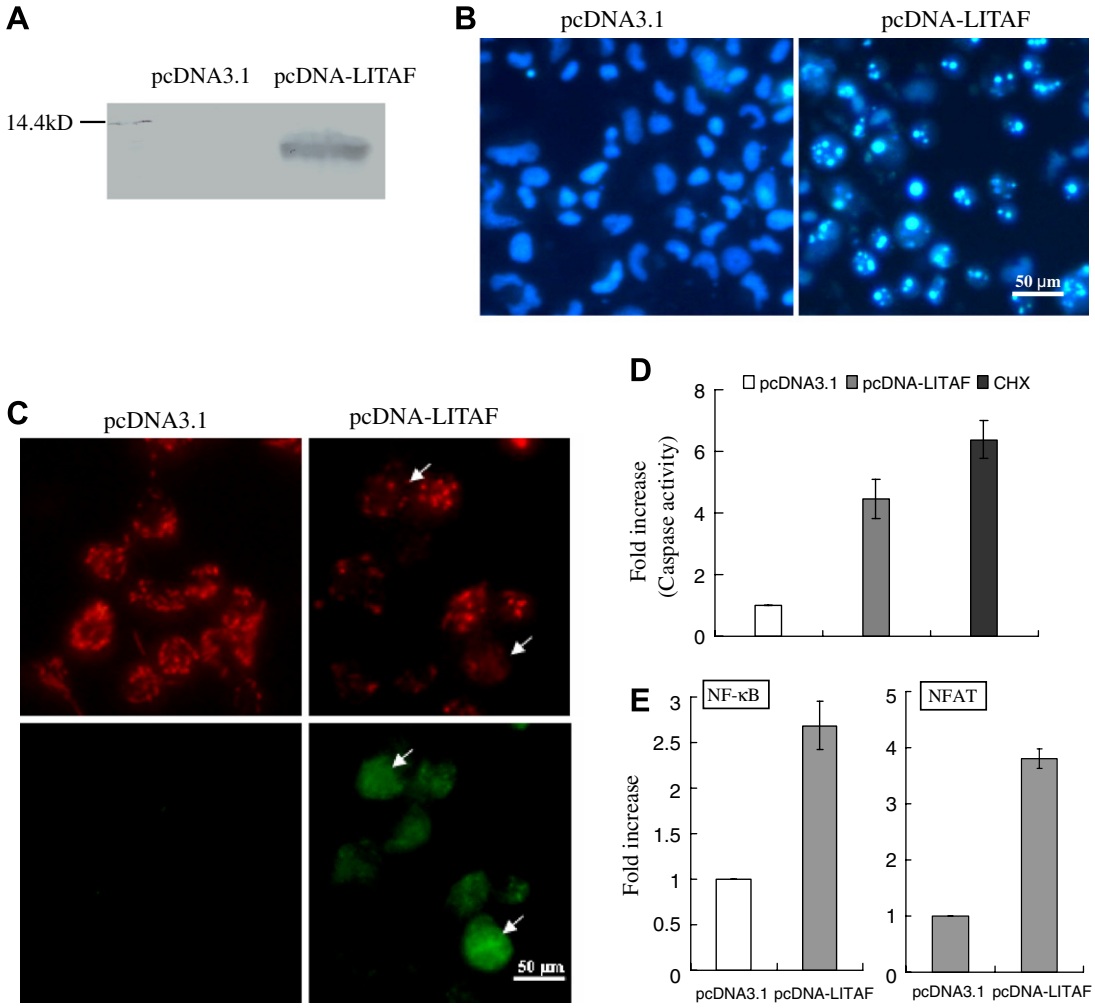

Fig. 4. Effects of SGIV LITAF expression on fish cells. (A) Confirmation of SGIV LITAF expression in transfected cells by Western blot. (B) Effect of SGIV LITAF overexpression on the nucleus morphology. Many apoptotic bodies were observed in pcDNA-LITAF transfected cells. (C) Effect of SGIV LITAF overexpression on $\Delta\Psi_m$ by fluorescence microscopy. The arrows show the loss of $\Delta\Psi_m$ cells, which switched from red to green fluorescence. (D) Measurement of caspase-3 activity in the pcDNA-LITAF or empty vector transfected cells. (E) Measurement of NF-κB and NFAT activity in the pcDNA-LITAF or empty vector transfected cells. In (D, E), the data are expressed as means ± standard deviation.

were only present in the sequenced genomes from the genus *Ranavirus*, but not in other larger DNA viruses so far sequenced. It is possible that LITAF may not be an essential gene for other iridoviruses, but may have some specific function during ranavirus pathogenesis.

To elucidate the function of SGIV LITAF, we analyzed its temporal expression pattern during in vitro infection. Combining detection of SGIV LIATF expression at transcription level, translation level, and under drug pressure, we deduce that SGIV LITAF is an early gene. The examination of the subcellular location of the protein revealed that the pEGFP-LITAF fusion protein was predominantly distributed in the cytoplasm and partly co-localized with mitochondria. Moreover, the immunofluorescence assay displayed the cytoplasmic distribution of SGIV LITAF after infection. Interestingly, SGIV LITAF appeared to aggregate toward the "virus factories" in some infected cells. Genome replication and assembly of iridovirus often take place in specific intracellular compartments known as "virus factories", and large clusters of mitochondria have been observed to distribute around the virus assembly sites during virus infection [16]. Similar results have been reported in cells infected with African swine fever virus [17]. Therefore, it is suggested that SGIV LITAF may be a protein that is associated with mitochondria. In addition, rounding-up of cells and apoptotic bodies were observed in pcDNA-LITAF transfected cultures, suggesting that SGIV LITAF expression could induce apoptosis.

Growing evidence suggests that apoptosis plays a critical role in viral pathogenesis, and virus encoded genes that trigger apoptosis have been identified gradually [18,19]. Recent studies indicated that iridovirus can induce apoptosis during infection [15,20,21]. Furthermore, our previous study also showed that SGIV infection could induce apoptosis, as indicated by Hoechst staining and TUNEL assay (data not shown). In the present study, JC-1 analysis showed that expression of SGIV LITAF could induce the collapse of $\Delta\Psi_m$. Caspase-3 activity was also heightened in the SGIV LITAF transfected cells. Considering that mitochondria are the central control point of apoptosis [22], and that changes in $\Delta\Psi_m$ are considered as an important event within the apoptosis cascades [23,24], we propose that the mitochondrion may be involved in LITAF-induced apoptosis. Viruses that induce apoptosis represent an important step in the spread of progeny to neighboring cells, while also evading the host immune and inflammatory responses [18]. Therefore, the current data suggest that apoptosis induced by SGIV LITAF, a protein encoded by the virus itself, may contribute to virus transmission during SGIV replication.

In addition, our results revealed that the activity of NF-κB and NFAT was increased in SGIV LITAF expressing cells. It has been shown that NF-κB and NFAT can regulate other genes related to cell cycle progression, cell differentiation, and apoptosis [25,26]. Given that these two transcript factors also contribute greatly to mediation of the immune response and are involved in virus replication and immune evasion [27], all these findings imply that SGIV LITAF may contribute to virus replication by exploiting apoptosis and regulating the host immune response. Future work will be directed to the elucidation of the role of SGIV LITAF in virus immune evasion.

Acknowledgments

This work was supported by grants from the National Basic Research Program of China (973) (2006CB101802), the National High Technology Development Program of China (863) (2006AA100306, 2006AA09Z445, 2006AA09Z411), and the National Natural Science Foundation of China (30700616, 30725027).

References

[1] T. Williams, V. Barbosa-Solomieu, V.G. Chinchar, A decade of advances in iridovirus research, Adv. Virus Res. 65 (2005) 173–248.
[2] Q.W. Qin, T.J. Lam, Y.M. Sin, H. Shen, S.F. Chang, G.H. Ngoh, C.L. Chen, Electron microscopic observations of a marine fish iridovirus isolated from brown-spotted grouper, *Epinepheous tauvina*, J. Virol. Methods 98 (2001) 17–24.
[3] Q.W. Qin, S.F. Chang, G.H. Ngoh-Lim, S. Gibson-Kueh, C. Shi, T.J. Lam, Characterization of a novel ranavirus isolated from grouper *Epinephelus tauvina*, Dis. Aquat. Organ. 53 (2003) 1–9.
[4] W.J. Song, Q.W. Qin, J. Qiu, C.H. Huang, F. Wang, C.L. Hew, Functional genomics analysis of Singapore grouper iridovirus: complete sequence determination and proteomic analysis, J. Virol. 78 (2004) 12576–12590.
[5] C.A. Benedict, T.A. Banks, C.F. Ware, Death and survival: viral regulation of TNF signaling pathways, Curr. Opin. Immunol. 15 (2003) 59–65.
[6] M.M. Rahman, G. McFadden, Modulation of tumor necrosis factor by microbial pathogens, PLoS Pathog. 2 (2006) e4.
[7] F. Myokai, S. Takashiba, R. Lebo, S. Amar, A novel lipopolysaccharide-induced transcription factor regulating tumor necrosis factor a gene expression: molecular cloning, sequencing, characterization, and chromosomal assignment, Proc. Natl. Acad. Sci. USA 96 (1999) 4518–4523.
[8] X.R. Tang, D.L. Marciano, S.E. Leeman, S. Amar, LPS induces the interaction of a transcription factor, LPS-induced TNF-alpha factor, and STAT6 (B) with effects on multiple cytokines, Proc. Natl. Acad. Sci. USA 102 (2005) 5132–5137.
[9] X. Tang, D. Metzger, S. Leeman, S. Amar, LPS-induced TNF-alpha factor (LITAF)-deficient mice express reduced LPS-induced cytokine: evidence for LITAF-dependent LPS signaling pathways, Proc. Natl. Acad. Sci. USA 103 (2006) 13777–13782.
[10] A.L. Bolcato-Bellemin, M.G. Mattei, M. Fenton, S. Amar, Molecular cloning and characterization of mouse LITAF cDNA: role in the regulation of tumor necrosis factor-alpha (TNF-alpha) gene expression, J. Endotoxin. Res. 10 (2004) 15–23.
[11] I.G. Woods, C. Wilson, B. Friedlander, P. Chang, D.K. Reyes, R. Nix, P.D. Kelly, F. Chu, J.H. Postlethwait, W.S. Talbot, The zebrafish gene map defines ancestral vertebrate chromosomes, Genome Res. 15 (2005) 1307–1314.
[12] Y.H. Hong, H.S. Lillehoj, S.H. Lee, D.W. Park, E.P. Lillehoj, Molecular cloning and characterization of chicken lipopolysaccharide-induced TNF-a factor (LITAF), Dev. Comp. Immunol. 30 (2006) 919–929.
[13] E.M. Park, Y.O. Kim, B.H. Nam, H.J. Kong, W.J. Kim, S.J. Lee, I.S. Kong, T.J. Choi, Cloning, characterization and expression analysis of the gene for a putative lipopolysaccharide-induced TNF-alpha factor of the pacific oyster, *Crassostrea gigas*, Fish. Shellfish. Immunol. 21 (2008) 11–17.
[14] H.E. Eaton, J. Metcalf, E. Penny, V. Tcherepanov, C. Upton, C.R. Brunetti, Comparative genomic analysis of the family Iridoviridae: re-annotating and defining the core set of iridovirus genes, Virol. J. (2007) 1–17.
[15] Y.H. Huang, X.H. Huang, J.F. Gui, Q.Y. Zhang, Mitochondrion-mediated apoptosis induced by *Rana grylio* virus infection in fish cells, Apoptosis 12 (2007) 1569–1577.
[16] X.H. Huang, Y.H. Huang, X.P. Yuan, Q.Y. Zhang, Electron microscopic examination of the viromatrix of Rana grylio virus in a fish cell line, J. Virol. Methods 133 (2006) 117–123.
[17] G. Rojo, M. Chamorro, M.L. Salas, E. Vinuela, J.M. Cuezva, J. Salas, Migration of mitochondria to viral assembly sites in African swine fever virus-infected cells, J. Virol. 72 (1998) 7583–7588.
[18] J.G. Teodoro, P.E. Branton, Regulation of apoptosis by viral gene products, J. Virol. 71 (1997) 1739–1746.
[19] A. Robert, M.J. Miron, C. Champagne, M.C. Gingras, P.E. Branton, J.N. Lavoie, Distinct cell death pathways triggered by the adenovirus early region 4 ORF 4 protein, J. Cell Biol. 158 (2002) 519–528.
[20] P.W. Lin, Y.J. Huang, J.A. John, Y.N. Chang, C.H. Yuan, W.Y. Chen, C.H. Yeh, S.T. Shen, F.P. Lin, W.H. Tsui, C.Y. Chang, Iridovirus Bcl-2 protein inhibits apoptosis in the early stage of viral infection, Apoptosis 13 (2008) 165–176.
[21] V.G. Chinchar, L. Bryan, J. Wang, S. Long, G.D. Chinchar, Induction of apoptosis in frog virus 3-infected cells, Virology 306 (2003) 303–312.
[22] S. Desagher, J.C. Martinou, Mitochondrial as the central control point of apoptosis, Trends Cell Biol. 10 (2000) 369–377.
[23] P. Marchetti, T. Hirsch, N. Zamzami, M. Castedo, D. Decaudin, S.A. Susin, B. Masse, G. Kroemer, Mitochondrial permeability transition triggers lymphocyte apoptosis, J. Immunol. 157 (1996) 4830–4836.
[24] D.R. LaJeunesse, K. Brooks, A.L. Adamson, Epstein–Barr virus immediate-early proteins BZLF1 and BRLF1 alter mitochondrial morphology during lytic replication, Biochem. Biophys. Res. Commun. 333 (2005) 438–442.
[25] G.P. Linette, Y. Li, K. Roth, S.J. Korsmeyer, Cross talk between cell death and cell cycle progression: BCL-2 regulates NFAT-mediated activation, Proc. Natl. Acad. Sci. USA 93 (1996) 9545–9552.
[26] J. Dutta, Y. Fan, N. Gupta, G. Fan, C. Gélinas, Current insights into the regulation of programmed cell death by NF-kappaB, Oncogene 25 (2006) 6800–6816.
[27] J. Hiscott, H. Kwon, P. Genin, Hostile takeovers: viral appropriation of the NF-kappaB pathway, J. Clin. Invest. 107 (2001) 43–151.